Target Helicity Correlations in GlueX

Letter of Intent

D. Keller,[‡]
University of Virginia, Charlottesville, VA 22903

F. J. Klein,
The Catholic University of America, Washington, DC 20064

W. K. Brooks,
Universidad Tecnica Federico Santa Maria, Valparaiso, Chil e

C. Keith,
Thomas Jefferson National Accelerator Facility, Newport News, V A 23606

[‡]Contact

Abstract

We express interest in measuring the set of polarized observables for pseudoscalar-meson and vector meson photoproduction using circularly and linearly polarized beams on a longitudinally polarized target. We suggest the development of a polarized target specialized for the GlueX configuration in order to study a broad range of polarized observables in the photon beam energy range between 5 GeV and 9 GeV. We are interested in using both a polarized proton and a polarized deuteron target. Though a polarized target system capable of longitudinal and transverse polarization is possible, we focus on longitudinal but ultimately expect to extract a full set of polarized observables. This includes single-polarization and beam-target, target-recoil, and beam-recoil double-polarization asymmetries, as well as tensor polarized observables, and initial state helicity correlations in possible exotic state hadrons. In this update to LOI 12-16-005, we focus on some of the longitudinally polarized target observables with $\gamma p \rightarrow K^+\Lambda$ and $\gamma n \rightarrow K^0\Lambda$. This experiment would be complimentary to previously proposed GlueX experiments, providing additional information to be used to determine complete isospin amplitudes and assist the search for exotic states.

Contents

1 Background

Over the last 15 years, there has been a gradual acceleration in the observation of new hadronic states that cannot be classified by the well-tested quark model of mesons and baryons. These manifestly exotic states with properties suggesting four or more quark and antiquark combinations are tools to explore the gluonic degrees of freedom. The spectroscopy of these states provide the quintessential test-bed of the assumptions in lattice QCD and the phenomenology leading to confinement.

The LHC experiments will not only continue to identify new and interesting states, but also continue to gain access to much larger data sets. Additionally, the BEPC collider will continue to collect data at relevant energies for studies of $c\bar{c}$ states. The Super-KEKB accelerator will also produce a large amount of data to the Belle II experiment. The FAIR experiment will be a key player at GSI in Germany using an antiproton beam to study exotic hadrons in the PANDA experiment. JLab hopes to provide insight into lower lying exotics and GlueX specifically intends to identify exclusive reactions in order to perform the amplitude analyses that will extract exotic meson J^{PC} quantum numbers in this unique energy region. Another distinguishing characteristic of JLab is its capacity to study the spin states, which are generally less accessible at other facilities. At this stage, it is still unclear as to what contribution GlueX will make to the search for exotics. However, it is clear that GlueX is incredibly well positioned to expand into a full polarized observable physics program.

Polarized observables exhibit very rich structure, offering access to the degree of complexity in production and polarization mechanisms. These tools add considerable sensitivity and information in each measurement and provide a much broader reach to explore the spectrum contributions, far beyond amplitude analysis alone. This additional information on the various contributions leading to the final state is crucial and will need to be fully exploited in the attempts to understand exotic contributions.

Photo-excitation of the nucleon, as seen in the hadronic spectrum, provides a critical approach for probing the quark and gluonic degrees of freedom, the nature of the confinement mechanism, possible gluon-gluon interactions, and the missing resonances. Exotic hybrid mesons manifest gluonic degrees of freedom and their detailed spectroscopy will provide the precision data necessary to test long-standing assumptions in the modern theoretical framework. The use of polarized photon beams with polarized targets provides the most information with a comprehensive set of constraints to assist in the search of exotic mesons, as well as an understanding of their backgrounds. Here we suggest the first steps in such a program by starting with the basic $K\Lambda$ channels, which are essential to fill in with missing observables up to the 9 GeV photon energy region. This should be thought of as a critical first step in launching an investigation to completely map out the competing channels in the spectrum with high precision and a multitude of constrains from as many observables as possible.

In general, higher mass resonances can overlap with significant interfering backgrounds from u-channel processes. Multivariate extraction techniques and detailed partial-wave analyses are invaluable, as are the constraints provided by the polarization of the target nucleons. The ideal frame-work would account for the coupling between the various meson-decay channels using as many polarized observables as can be achieved. A comprehensive investigation of amplitudes and

phase transitions is required for both the meson and baryon spectrums, which is chiefly determined from πN reactions. This will assist in the deconvolution of the spectrum in the search for and study of the pattern of gluonic excitation in the meson spectrum. Using polarized target data with unpolarized target data, in combination with various beam helicities, optimizes information extraction. The measurement of double spin polarization asymmetries can reveal information on the nucleon hidden structure, hadron photoproduction dynamics, and exotic hadron property. The expected dominance of the one-pion-exchange, which fixes naturality in the t-channel for some typologies, can enable, by means of polarization observables, discrimination between naturalities of the resonances produced. If there are limitations in the partial wave analysis (PWA) it is sometimes possible to find maxima in the angular distributions of the decay products, which are dominated by a single resonance of interest.

The enhancement of the hadronic interactions at threshold implies that new types of charm-based resonances may form in photoproduction in the available energy range. Some of the possibilities are the J/ψ-nucleon resonances at threshold in reactions such as $\gamma p \rightarrow [J/\psi p]$, $\gamma p \rightarrow [J/\psi p]\gamma$, $\gamma p \rightarrow [J/\psi]\pi^+$, and with the deuteron target $\gamma d \rightarrow \bar{D}^0 + [\Lambda_c n]$ and $\gamma d \rightarrow [\Lambda_c] + [\bar{D}^0 n]$ reactions. An additional possibility is the octoquark $|uuduudc\bar{c}>$ in γd. In each case, resonance formation implies strong spin correlations. We have also started an effort on some open charm and J/ψ channels in Hall C to take advantage of the high intensity compact photon source (CPS) [1]. For channels with smaller polarized cross sections the unique combination of high photon intensity (10^{12}) and polarized target in Hall C can significantly compliment a Hall D polarized target effort. the previous Hall D Letter of Intent (LOI 12-16-005) to Hall C to take advantage of the high intensity compact photon source (CPS) [1]. It is for this reason that several of the aforementioned channels from the original letter of intent (LOI 12-16-005) are no longer used to directly motive here.

1.1 Overview

There is a great deal to learn about in the photon energy range of 5-9 GeV, and GlueX now benefits from expanding to a full hadron spectroscopy and N^* program. As previously mentioned, there is a growing body of evidence for exotic state candidates from other facilities in recent years but there are no accompanying claims from Hall D. There are, however, publications of beam asymmetries and many additional interesting measurements the will be released in the near future. From the data so far, in addition to the expected light meson spectroscopy is the J/ψ photoproduction near threshold. This charmonium production can provide much needed information on gluonic structure and could potentially allow a direct study of various exotic states observed at LHCb. Much, much more information is needed.

To a large extent, the initial Hall D experiments were necessary before starting to think about what sort of polarized target program would not only best compliment the current effort , but also help to determine what decay channels would benefit most from additional polarized observables. At this stage, it is clear that there is independently there exists a lot of physics that comes from using a polarized target in GlueX. Here, we suggest the first of many polarized target runs using both longitudinally polarized deuteron and proton targets. We also continue interest in a transversely polarized target and continue to work on optimization of such a configuration for Hall D, consid-

ering the background magnetic field. There is a great deal to explore in both pseudoscalar and vector meson production and GlueX has the potential to add a considerable amount to the world's data of polarized observables. The observation of the expected well-know meson resonances in recent GlueX runs, as well as the first successful reconstruction of the J/ψ demonstrates considerable potential. The addition of the DIRC detector will also improve this potential by adding an improved π/K separation [2]. With the additional factor of five or more in luminosity, we believe that now is the time to reconsider a proposal for a polarized target. With these recent developments we reassert our interest in a polarized target physics program in Hall D. The Hall D energy range and the advancement in polarized target technology at JLab and UVA gives Hall D the opportunity to greatly increase its physics output for years to come.

2 Polarization Observables

In the search for exotic mesons, polarized target data should be taken to acquire the most information on the amplitudes and phase contributions seen in the spectrum. Confirmation of any $J^{p,c}$ states in the unpolarized target GlueX runs will be critical, and polarized target information can be used to provide additional constraints. This information can also be helpful in the separation of exotics from non-trivial gluonic constructions of non-exotic hybrid mesons. The polarized target observables help to make a more *complete* measurement for a given topology. The masses and quantum numbers are not only essential to the measurement of exotic states but also to the phenomenology that may arise from NN^*-exotic couplings. An intimate understanding of the background can be acquired for many channels by adding constraints over phase space through the study of the polarized observables. For example, the polarized observables for the processes $\gamma N \to \pi\pi N$ and $\pi N \to \pi\pi N$ were developed [3] by using both a helicity and hybrid helicity-transversity basis. Such observables are crucial if the processes that produce final states consisting of a spin-1/2 baryon and two pseudoscalar mesons are to be fully investigated in hadron spectroscopy. In general, the S, P_0, P_+, and P_- amplitudes and their relative phases depend on the nucleon helicities. Without using a polarized target, these partial waves cannot be deduced from the moments without further assumptions [4, 5]. Unambiguous solutions do not exist in these instances and additional assumptions are necessary in the absence of these additional observables.

In photoproduction, the one pion exchange mechanism dominates, which prefers spin flip at the nucleon vertex. Under these conditions, the rank of the spin-density matrix is reduced to one and all density matrix elements can be fixed. Therefore, in [6] it was assumed that for small values of t, the proton spin-flip amplitude is dominant. On broader terms, it is assumed that the $\pi\pi$ phase does not depend on the projection of the orbital angular momentum onto the flight direction with which it is produced (phase coherence); and that the ratio of flip and non-flip amplitudes is universal (spin coherence). For large t, neither phase nor spin coherence is granted, and feed-through of higher partial waves into the scalar wave cannot be excluded without exploiting a polarized target. The greatest amount of information gain will come from searching for exotic hadron states while mapping the coupled-channel background. This is best executed with wide kinematic coverage and many polarization observables. In the next few sections, we will discuss some of the polarized observables achieved using the suggested configuration of a polarized target.

2.1 Pseudoscalar Mesons

The measurements of photoproduction of pseudoscalar mesons have really just begun at JLab; and it is expected the sector will provide much more information by extending the energy range up 9 GeV. It is still possible to discover new states that couple to other decay channels such as $\pi\pi N$, ρN, ωN, ηN, $K\Lambda$ or $K\Sigma$. The KY channels mentioned here are considerably important in that they are the most well-understood, strange, pseudoscalar channels that are still in need of complete data. This is especially true for $\gamma n \rightarrow K^0 Y$. In such an experiment, to measure KY polarized observables there is nothing that precludes us from measuring both the single and double polarization asymmetries in π, η, η' and D as well. The decay properties of the pseudoscalar mesons are a bit contradictory to the mass hierarchy. In particular, this applies to the large component of strange and anti-strange quarks in the η than the η'. The next excited state $\eta(1405)$ may suggest that the η and η' mix with the pseudoscalar glueball, which should occur, in its pure state, above the scalar glueball in mass. Also, polarization effects in the photoproduction of the pseudoscalar $\bar{D}$ charmed mesons in exclusive processes $\gamma + N \rightarrow Y_c + \bar{D}$ with a circularly polarized photon should lead to nonzero polarization of the Y_c-hyperon with $x-$ and $z-$components and non vanishing asymmetries using a polarized target. There is a lot to study near threshold and very little polarized target data presently available. Needless to say, coupled-channel PWA are needed to understand interferences on several interesting channels. Both more data on many channels and many observables are required, preferably in an experiment that can take the data simultaneously on multiple observables to reduce systematics.

The pseudoscalar meson photoproduction experiments have lead the search for states in the spectrum suggested by lattice solutions of QCD. Though many experiments to investigate the polarized observables and search for weak resonances have been led (some at JLab E03-105, E01-104, E05-012, E06-013, and E06-101), there is still significant data needed. In order to build a good understanding of the pseudoscalar meson landscape for GlueX, it is necessary to extend the kinematic range (up to W=3.2 GeV) of the observables using a polarized proton and neutron target in order for information to be acquired on the photo-couplings to I=1/2 states needed to explore the mechanisms for resonance excitation.

There still exists extensive missing resonances as compared to the predictions of the Quark models [7, 8] which would usually be required to more fully account for the baryon pressure during the chiral phase transition. Polarized observables add clarity to this search and a lot of this type of experimental information has come from the πN reactions, which are described by two complex spin-dependent amplitudes. There is very little data on the double-polarization asymmetries.

Photoproduction of pseduoscalar mesons can be used to obtain a large number of polarized target observables on both the polarized proton and neutron targets. The two spin states of the photon and the nucleon lead to four complex helicity amplitudes that determine single-pseudoscalar ($J^\pi = 0^-$) meson production from the neutron target, and four from the proton target. There are eight quantities to be determined for each target isospin by measuring different observables. In addition to the unpolarized cross section, there are three single-spin asymmetries accessed by polarizing the beam (Σ), the target (T), or the recoiling baryon (P); as well as three sets of double-polarization asymmetries corresponding to the beam-target (BT), target-recoil (TR), and beam-recoil (BR) combinations. A complete data set that eliminates discrete ambiguities requires a

minimum of eight observables, which include the unpolarized cross section, the single-spin asymmetries (Σ, T, P), and four double-polarization asymmetries, at least one involving recoil polarization. Ideally, even a greater number of alternative observables is desirable to mitigate the effects of systematic uncertainty in a PWA. Triple-polarization data for single-pseudoscalar meson production can provide additional determination for other observables.

For the present letter of intent, we choose to focus on $\gamma p \rightarrow K^+\Lambda$ and $\gamma n \rightarrow K^0\Lambda$ though for each target there are several πN, KY channels that can be measured simultaneously. In the case of the kaon production, the angular distributions in the weak hyperon decays will be used to determine recoil polarization.

Theoretical work was initiated some time ago and then experienced a surge largely induced by the JLab Excited Naryon Analysis Center (EBAC), which had extended the Sato-Lee model to the higher mass N^* region with a dynamical coupled-channel model [9]. Other work to develop the dynamical coupled-channel calculation that describes the γN, πN and $K\Lambda$ channels and their interactions was also explored [10, 11]. In fact, the EBAC worked extensively on dynamical coupled-channel analysis of similar typologies and their connection to Hadron Models and Lattice QCD up until roughly 2011.

Comparisons to predictions can yield complications through the dressing of the interaction vertices. A resonance is associated with pole in an s-channel diagram with significant particulars deep in the verticies. Hyperon channels of interest can be either produced directly $\gamma p \rightarrow K\Lambda$ or from the multi-step $\gamma N \rightarrow \pi N \rightarrow KY$ processes which can have effects of channel coupling turn off reverting to *tree-level* processes. This implies that calculating the strong vertex becomes a multichannel, multi- resonance task, with Unitarity requirement connecting all possible channels. These coupled-channel dressings of the strong vertex essentially determine the spectral properties of N^* [12].

Improved determination of neutron photo-couplings was proposed in experiment E06-101, which was the $g14$ run in Hall B. Measurements on the beam-target double polarization asymmetry have been published [13] with other work soon to come. The main subtleties of the impact of the new polarization data on multiple analysis using a polarized neutron target are discussed using the polarized HD in CLAS and are discussed in [12]. Though a successful experiment, there are limited statistics and a limited kinematic range. Meson photoproduction requires eight of sixteen possible observables to determine their spin-dependent amplitudes with the ideal scenario being over-constrained to significantly reduce systematics. By taking significantly more data and extending the photon energy up to 9 GeV there is no doubt that new N^* candidates will emerge and a more complete understanding of the pseudoscalar meson spectrum will be achieved.

2.1.1 Polarized Proton Target

Circular polarized beams can be used to measure the E beam-target asymmetry and the $C_{x'}$ and $C_{z'}$ beam-recoil asymmetries (in-plane recoil components), and linearly polarized photon beams can be used to measure the single-spin beam asymmetry defined as Σ, the G beam-target asymmetry, the $O_{x'}$ and $O_{z'}$ beam-recoil (in-plane component) asymmetries, and the single-spin target asymmetry T, a beam-recoil observable. Combining all beam polarization states will provide measurements of the Λ recoil single-spin asymmetry, P, and the target-recoil observables $L_{x'}$ and $L_{z'}$ (in-plane

Photon			T			R				+	
	-	-	-	-	x'	y'	z'	x'	x'	z'	z'
	-	x	y	z	-	-	-	x	z	x	z
Unpolarized	σ_0	0	T	0	0	P	0	$T_{x'}$	$-L_{x'}$	$T_{z'}$	$L_{z'}$
Linearly Pol.	$-\Sigma$	H	$(-P)$	$-G$	$O_{x'}$	$(-T)$	$O_{z'}$	$(-L_{z'})$	$(T_{z'})$	$(-L_{x'})$	$(-T_{x'})$
Circularly Pol.	0	F	0	$-E$	$-C_{x'}$	0	$-C_{z'}$	0	0	0	0

Table 1: Polarization observables in photoproduction of pseudoscalar mesons. The entries in brackets denote polarization observables which also appear elsewhere in the table. Here T is target, R is recoil, and + is target and recoil.

components). Finally, triple beam-target-recoil measurements with linearly polarized photons will access the transverse-Target-Recoil asymmetries $T_{x'}$ and $T_{z'}$.

The polarization observables [14] in photoproduction of pseudoscalar mesons are related to the photon beam, target, and recoil polarization states in Table 2.1.1. There are 16 different polarization observables for real photon experiments. The differential cross section can be classified by 3 classes of polarization experiments. For a polarized photon with a polarized proton target, the cross section is expressed as:

$$\begin{aligned} \frac{d\sigma}{d\Omega} &= \frac{d\sigma_0}{d\Omega}[1 - P_{lin}\Sigma\cos 2\varphi \\ &+ P_x(-P_{lin}H\sin 2\varphi + P_\lambda F) \\ &- P_y(-T + P_{lin}P\cos 2\varphi) \\ &- P_z(-P_{lin}G\sin 2\varphi + P_\lambda E)], \end{aligned} \tag{1}$$

where σ_0 is the unpolarized differential cross section, P_{lin} is the transverse photon polarization, P_λ is the (right-handed) circular photon polarization, and ϕ is the angle between photon polarization vector and reaction plane. The polarization states of the target proton and recoiling baryon are denoted by $P_{x,y,z}$ and $R_{x',y',z'}$ respectively. For polarized photons and recoil polarization:

$$\begin{aligned} \frac{d\sigma}{d\Omega} &= \frac{d\sigma_0}{d\Omega}[1 - P_{lin}\Sigma\cos 2\varphi \\ &+ P_{x'}(-P_{lin}O_{x'}\sin 2\varphi - P_\lambda C_{x'}) \\ &- P_{y'}(-P + P_{lin}T\cos 2\varphi) \\ &- P_{z'}(P_T O_{z'}\sin 2\varphi + P_\lambda C_{z'})]. \end{aligned} \tag{2}$$

For polarized target and recoil polarization, the cross section can be expressed as:

$$\begin{aligned} \frac{d\sigma}{d\Omega} &= \frac{d\sigma_0}{d\Omega}[1 + P_{y'}P + P_x(P_{x'}T_{x'} + P_{z'}T_{z'}) \\ &+ P_y(T + P_{y'}\Sigma) - P_z(P_{x'}L_{x'} - P_{z'}L_{z'})]. \end{aligned} \tag{3}$$

2.1.2 Polarized Deuteron Target

For the polarized beam and a polarized deuteron target, the cross section for single-pseudoscalar meson production can be expressed as:

$$\begin{aligned}\frac{d\sigma}{d\Omega} &= \frac{d\sigma_0}{d\Omega}[1 + P_\gamma^L\left(\Sigma + \frac{1}{\sqrt{2}}P_D^T T_{20}^L\right)\cos 2\varphi \\ &+ P_\gamma^L P_D^V G \sin 2\varphi \\ &- P_\gamma^C P_D^V E + \frac{1}{\sqrt{2}}P_D^T T_{20}^0].\end{aligned} \tag{4}$$

Here P_D^V is the vector polarization of the deuteron along the beam axis, P_D^T is the deuteron tensor polarization, P_γ^C and P_γ^L are the circular and linear photon polarizations, respectively, and φ is the angle between the linear photon polarization and the reaction plane. Two additional Tensor asymmetries T_{20}^L and T_{20}^0 can be measured by optimizing the tensor polarization of the spin-1 target while minimizing the vector polarization. In addition, the tensor polarization can be minimized when taking data for the vector polarization observables. The manipulation of vector and tensor polarization using RF-irradiation has been the focus of recent solid polarized target research at the University of Virginia. This will be discussed further in Section 3.

For the case of polarized beams and an analysis of recoil hyperon polarization, the cross sections are:

$$\begin{aligned}\frac{d\sigma}{d\Omega} &= \frac{d\sigma_0}{d\Omega}[1 + P_\gamma^L\left(\Sigma - P_r^y T\right)\cos 2\varphi \\ &- P_\gamma^L\left(P_r^x O_{x'} + P_r^z O_{z'}\right)\sin 2\varphi \\ &- P_\gamma^C\left(P_r^x C_{x'} + P_r^z C_{z'}\right) \\ &+ P_r^y P].\end{aligned} \tag{5}$$

The dependence on target and recoil polarization is given by:

$$\begin{aligned}\frac{d\sigma}{d\Omega} &= \frac{d\sigma_0}{d\Omega}[1 - P_D^V\left(P_r^x L_{x'} - P_r^z L_{z'}\right) \\ &+ P_r^y P \\ &+ P_\gamma^L P_D^V (P_r^x T_{z'} - P_r^z T_{x'})\sin 2\varphi].\end{aligned} \tag{6}$$

And finally, considering polarized beams and logitudinal target polarization, the cross section is,

$$\begin{aligned}\frac{d\sigma}{d\Omega} &= \frac{d\sigma_0}{d\Omega}[1 + P_\gamma^L\left(I^c + P_D^V P_z^c\right)\cos 2\beta \\ &+ P_\gamma^L\left(I^s + P_D^V P_z^s\right)\sin 2\beta \\ &+ P_\gamma^C\left(I^o + P_D^V P_z^o\right) + P_D^V P_z].\end{aligned} \tag{7}$$

The I^c observable is the analog of the beam asymmetry and the P_z^s and P_z^o asymmetries are the 2π analogs of the G and E observables. The new developments in RF spin manipulation on the tensor polarization will allow for direct extraction of the tensor observables, as well as to mitigate these terms when measuring the others.

2.1.3 The Central Proposed Measurement

The suggested experiment would tag a circularly polarized photon beam produced by the bremsstrahlung of longitudinally polarized electrons and linearly polarized photons from a coherent bremsstrahlung in diamond crystals. The polarized target would be a frozen-spin hydrogen and deuterium target system, similar to the CLAS FROST target but optimized for the Hall D geometry, background field, and target length. This focus provides a base channel to build from. There are many pseudoscalar meson channels that can be very interesting to study with a polarized target. The π, η, and η' all currently lack complete polarized target data at the Hall-D photon energy range.

2.2 Vector Mesons

The photoproduction of vector mesons (ρ, ω, ϕ) should also be considered an important part of the experiment. With a polarized beam and target, it is possible to explore the dynamics of basic hadron structure. The analysis of all possible polarization observables for the case of vector mesons photoproduction from a nucleon target is presented. The polarized target observables are needed to completely determine the basic photoproduction amplitudes and the relationships between spin observables and the formation of resonances. Acquiring extensive data on the angular dependence of spin observables, especially near thresholds and resonances, is critical for understanding the vector mesons.

For the case with a polarized deuteron target, we get additional observables from the tensor polarization observables, which can play a significant role in understanding all possible solutions to the exotic channels in the spectrum with unnatural parity exchange ($s\bar{s}$-knockout) in the photoreaction with a neutron. We believe the avenue has much physics to explore on its own and deserves further development. For now, we quickly summarize some of the more popular and traditional points.

2.2.1 ϕ-Mesons Production

Measurement of double polarization asymmetries for ϕ photoproduction with the polarized target and a polarized photon beam is a sensitive means to investigate small and exotic amplitudes, such as an $s\bar{s}$-quark content of nucleons via interferences with dominant amplitudes and the determination of the spin value of produced hadrons such as the pentaquark. In order to realize the double polarization measurements to study the $s\bar{s}$-quark content, as well as exotic hadron structures, the processes $\gamma p \rightarrow K^* Y$ and $\gamma p \rightarrow \phi p$ should be studied in the Hall-D accessible photon energy range. Some polarization observables in vector meson photoproduction are discussed here [15, 16].

For coherent photoproduction from the polarized deuteron using circularly-polarized photon-beam, there are three initial spin states with total spin projection: $J_z = 2$ when the deuteron is polarized along the beam polarization, $J_z = 0$ when the deuteron is polarized along the opposite direction to the beam polarization, and $J_z = 1$ when the deuteron is polarized perpendicular to the beam polarization. This leads to three beam-target asymmetries C_{BT}^{21}, C_{BT}^{20}, and C_{BT}^{10}. From [17], the amplitude of the photoproduction deuteron is proportional to the product of the elementary isoscalar amplitude and the deuteron form factors, which differ for the processes with *natural* and

unnatural parity properties. The amplitudes decrease fast with $-t$ due to the effect of these form factors. The unnatural parity-exchange transitions are suppressed for the deuteron in the tensor polarized target with spin projection $M_i = 0$. The form factors of the natural parity-exchange (Pomeron) amplitudes with spin projections $M_{i,f} = \pm 1$ and $M_{i,f} = 0$ are distinct and both differ from the *unnatural* parity-exchange form factor. Tensor target optimization applicable to this type of solid polarized target is discussed in Section 3. See also the research presented in [18].

For the incoherent photoproduction from the deuteron, the total amplitude is a coherent sum of the photoproduction from the proton and the neutron. The interference term between these two amplitudes in a deuteron is proportional to the linear combination of the deuteron form factor. For the polarized deuteron target, there are three beam-target asymmetries analogous to the coherent photoproduction observables already mentioned. These can be used in combination with analysis of the photoproduction from the proton, leading to unique solutions to the exotic channels with unnatural parity exchange ($s\bar{s}$-knockout) in the photo-reaction with a neutron.

There are many ϕ meson production channels that are worthy of polarized target investigations at the Hall-D photon energies, such as $\gamma p \to \phi p$, $\gamma d \to \phi d$, $\gamma d \to \phi pn$. Hall-D can now cover the photon energy region not yet studied by past experiments. This data will be complimentary to Hall-B Frozen spin g8, g9, and HD-ice g14 at 6 GeV, as well as the low q^2 12 GeV proposals on HD-ice along with the LEPS HD-ice data. Here we expect to cover a larger kinematic range with higher statistics than the present Hall-B proposal with high polarization for the proton and deuteron vector and tensor polarizations. In addition, greater sensitivity to the tensor polarized observables can be achieve with a RF-manipulated Frozen spin target.

2.2.2 ω-Mesons Production

The theoretical interpretation of cross-section data for $\gamma N \to \omega N$ [19, 20, 21, 22, 23] indicates dominant t-channel production from unnatural parity exchange (π^0 and possibly η) at low energies, natural parity exchange (pomeron) at higher energies, and sizeable nucleon u-channel contributions. The relative strength of competing natural and unnatural parity-exchange processes can in principle, be extracted using plane-polarized photons [24], which is a project that is of particular interest in the photon energy range of Hall D to map out the transition from unnatural to natural parity exchange. Additional target polarization provides double-polarization observables C_{BT}^{ij}, which are crucial when performing the separation in the presence of u-channel (nucleon-pole) contributions, with C_{BT}^{zy}, C_{BT}^{zz} changing signs in backward direction for u and unnatural parity exchange [25, 26]. Moreover, the observables C_{BT}^{xy}, C_{BT}^{xz} vanish for all production angles [26]. Detailed investigations of these contributions are feasible with the proposed polarized target inside the GlueX detector.

3 The Polarized Target

This experiment will use a new Hall-D frozen spin target dilution refrigerator constructed to fit into the GlueX detector, see Fig. 1. The target is typically polarized at a higher temperature $\sim$1K and set in frozen spin mode by running at lower temperature $\sim$30 mK. The cooldown of the magnet from room temperature to 4 K takes about 6 hours. The dilution refrigerator is then cooled in 2

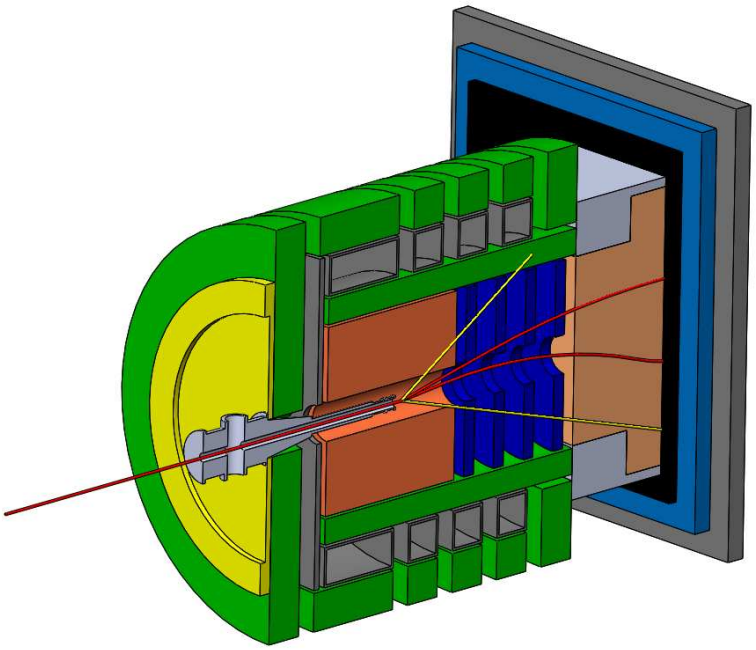

Figure 1: A Frozen Spin Target fitted into GlueX.

hours to 1 K, the cells of the target holder are filled with the material, and the target holder is pushed into the precooled mixing chamber. Purging, final cooldown, and condensing the ^{4}He-^{3}He mixture takes less than 1 hour. During DNP the temperature of the helium mixture decreases slowly from about 350 mK to 200 mK as the optimum microwave power is reduced with increasing polarization. The expected DNP vector polarization is greater than 80%, which can be a bit greater for negative polarization. A full polarization build-up using DNP usually takes about 12 hours. The target is cooled down below 100 mK by turning the microwave power off 0.5-1 hours before the field rotation. The ultimate temperature is reached only after several hours of running without microwaves. After circulating the ^{3}He for several minutes, the fridge will begin to dilute, and the temperature gradually drops to about 30 mK.

The fridge should be of cooling power comparable to the previous Hall-B dilution fridge with a target cell of approximately 7 cm. The fridge will be designed specifically for fitting into the GlueX detector. A diagram of the inter workings of the Hall-B frozen spin target can be seen in Fig. 1.

Figure 3 shows the NMR signal and polarization growth curve of deuterated propanediol doped with OXO63. Irradiated d-butanol is expected to perform on a similar level.

3.1 Tensor Polarization Manipulation

Deuteron spin alignment can be manipulated when exposed to a modulated RF field using an external coil around the target cup. The accuracy and enhancement of the tensor polarization greatly dependents on the polarization technique. Tensor polarization can be measured when the magnetic

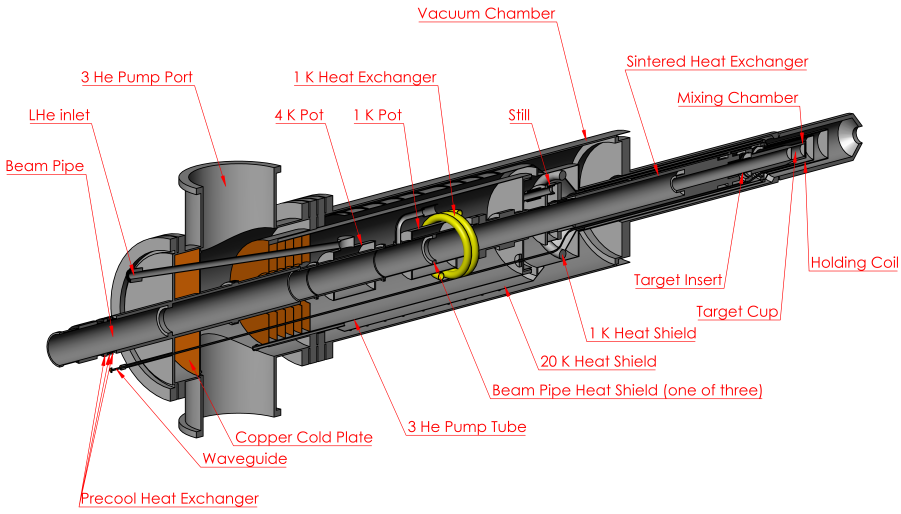

Figure 2: Cross section view of a FROST target fridge, with the overall length of the cryostat is approximately 2 m.

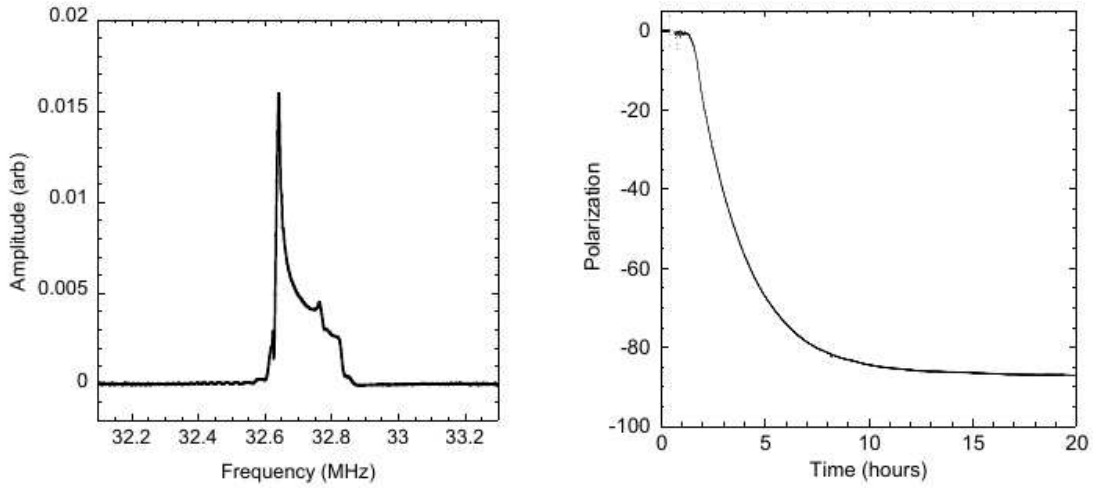

Figure 3: Performance of the signal and polarization growth curve of deuterated propanediol doped with OXO63 from Jlab Hall-B FROST experiment.

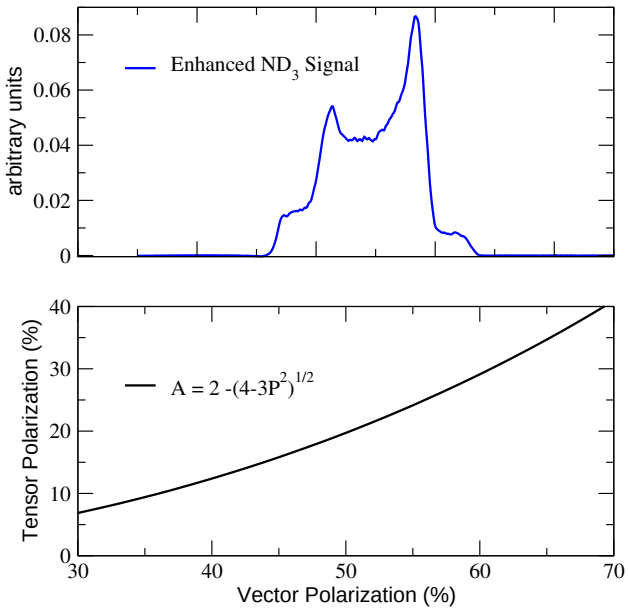

Figure 4: **Top**: NMR signal for ND_3 with a vector polarization of approximately 50% from the GEN experiment. **Bottom**: Relationship between vector and tensor polarization in equilibrium, and neglecting the small quadrupole interaction.

sublevels are out of the Boltzmann distribution, when the intensities I_+ and I_- of each peak in the NMR signal represent the total area of each independent transition probability distribution. The tensor polarization under any spin distribution can be described as:

$$P_{zz} = C(I_+ - I_-). \tag{8}$$

Here C is the calibration constant. A positive tensor polarization enhancement occurs only when the $n_+ + n_-$ population increases with respect to n_0 population. To optimize positive tensor polarization, the vector polarization must be maximized using DNP, at which point the microwave is turned off and the RF-modulation begins. The RF-modulation induces transition at the frequency domain that it spans. Tensor polarization optimization will occur when the range in RF-modulation is chosen to maximize the difference in the intensities I_+ and I_- throughout the signal.

Negative tensor enhancement can be achieved by proton deuteron cross-polarization, which fills the $m = 0$ sublevel directly from the spin reservoir of another (proton) system [27]. The deuteron spin system is polarized using strong thermal contact between the proton spin-spin interaction reservoir and the deuteron quadrupole interaction reservoir. The thermal contact is maintained using high powered RF just off of the Larmor frequency of the two spin species. As the $m = 0$ sublevel is filled, there are transitions of equal likelihood to the greater or lesser energy levels, so the NMR signal using this type of cross polarization both absorption and emission. The greater the proton spin-spin reservoir, the greater the tensor polarization achievable in the deuteron. This can be done to achieve a near zero vector polarization, however, the maximum tensor polarization that can be acquired for the thermal conditions of the Duke/UVA cryostat has yet to be

studied. Measuring and fitting techniques for RF manipulated deuteron NMR lines have been developed recently at UVA. In addition, RF techniques that can optimize tensor polarization for a specific experimental requirement have also been explored [18].

A selective AFP (Adiabatic Fast Passage) can also be used to achieve negative tensor polarization. An AFP [28, 29] is a reverse in the polarization using a single RF sweep which is slow enough to follow the Adiabatic Theorem but still fast with respect to the relaxation rates of the material at the temperature and field conditions. The spins effectively follow the magnetic field of the RF sweep as it passes through the resonance line, resulting in a helicity flip of the target. A selective AFP is when the RF is swept through a specific frequency domain to selectively manipulate the deuteron alignment. UVA has recently achieved this with d-butanol at 5 T and 1 K.

Negative tensor polarization is especially interesting because not only is it easier to hold zero vector polarization, but also the magnetic sublevels $m = +1$ and $m = -1$ are depleted to both fill the $m = 0$ sublevel, leading to a magnetization reservoir that is twice as large. This doubling of the polarization reservoir is only useful when the target state can be held long enough to take data in an experiment. This is easily achieved when using a Frozen Spin Target where the temperature of the material is held below 100 mK, which slows the relaxation rates, effectively freezing the polarization in place.

4 Beam Time Estimate

Though there are several interesting things to explore here, we choose $\gamma N \rightarrow KY$ to estimate the beam time. We expect that for a polarized target of 15 cm, we will get approximately $1.5{\times}10^5$ events day that can contribute to the asymmetry of interest using $10^7\gamma/s$ for 1 μb cross section. We use E (*beam-helicity* asymmetry) to estimate the asymmetry precision for a 40 day run and expect that we will get similar precision for the other polarized target observables. The *beam-helicity* asymmetry is:

$$E = \frac{1}{P_\gamma P_T}\frac{\sigma_A - \sigma_P}{\sigma_A + \sigma_P}. \tag{9}$$

We use a photon polarization (P_γ=80%) and a target polarization of (P_T=70%). We estimate that for $W = 2.1$ GeV the total cross section is around 0.02 μb and at $W = 3.2$ GeV but drops with increasing W. To a crude approximation, we expect a statistical error of less than ± 0.01 if we divide the data into 10 polar angle bins from 5 to 150 degrees.

We expect that the systematic uncertainty for this experiment to be of the order of 6%, depending on the particular target and observable. We expect the target polarization measurement and the dilution factor to carry the majority of this, and there is about a 2% uncertainty in the beam polarization. We expect detector performance and background contamination to be less than 2% using the necessary analytical techniques.

A more complete estimate of rates and uncertainties can be provided after a detailed Monte Carlo study.

5 Summary

This letter of intent solicits approval to develop a full proposal to measure the full set of polarized observables for pseudoscalar-meson and vector meson photoproduction. We suggest the development of a polarized target designed specifically for the GlueX geometry to study a broad range of polarized observables in the photon beam energy range between 5 GeV and 9 GeV. We are interested in using both a polarized proton and a polarized deuteron target.

With encouragement from the PAC, we will write a formal proposal motivated by building upon the historic JLab N^* program while gathering additional information in the search for exotic states. There is significant opportunity to further the GlueX physics output with the use of a polarized target to gain information on a broad range of polarized observables in the available photon beam energy. We are interested in using a polarized proton and a polarized deuteron target with both linear and circularly polarized photon beams. A frozen spin target capable of longitudinal and transverse polarization offers the most physics but this effort will likely be broken up with the longitudinally polarized target being the initial focus. However, in the long run, we expect to be able to take transversely polarized target data as well. In this way it is necessary to design the fridge and magnets for optimal kinematic coverage to work with the Hall-D configuration of GlueX. A large set of polarization observables will be determined, including single-polarization and beam-target, target-recoil and beam-recoil double-polarization asymmetries, as well as tensor polarized observables, and initial state helicity correlations in possible exotic state hadrons. This experiment is complimentary to previously proposed GlueX experiments, providing additional information to be used to determine compete isospin amplitudes and assist in the search for exotic states.

Our crude estimates of beam time suggest that significant physics data can be collected in a reasonable amount of time and we expect to further develop the physics and fully list the possible channels to be explored in the full proposal. With encouragement from the PAC to move forward, we will connect with the GlueX collaboration to bring this project to fuition.

References

[1] E. Chudakov *et al.*, CPS-JLab **01**, (2019).

[2] J. Stevens *et al.*, JINST **11**, 07, C07010 (2016).

[3] W. Roberts and T. Oed, Phys. Rev. **C71**, 055201 (2005).

[4] W. Ochs, Nuovo Cim. **A12**, 724 (1972).

[5] P. Estabrooks and D. Martin, Phys. Lett. **B41**, 350 (1972).

[6] B. Hyams, Nucl. Phys. **B64**, 134 (1973).

[7] W. R. S. Capstick, Phys. Rev. D **58**, 074011 (1998).

[8] G. G. H. G.-T. R. Bilker, J. Ferretti, Phys. Rev. D **94**, 074040 (2016).

[9] T. S. A. Matsuyama and T.-S. H. Lee, Phys. Rept. **439**, 193 (2007).

[10] T.-S. L. B. Juli-Daz, B. Saghai and F. Tabakin, Phys. Rev. C **73**, 055204 (2006).

[11] T. Mart, Phys. Rev. C **62**, 038201 (2000).

[12] A. Sandorfi, Few-Body Syst **60**, 10 (2019).

[13] D. Ho *et al.*, Phys. Rev. Lett. **118**, 242002 (2017).

[14] G. Knochlein, D. Drechsel, and L. Tiator, Z. Phys. **A352**, 327 (1995).

[15] W. Pichowsky, S. Cetin, and F. Tabakin, Phys. Rev. **C53**, 593 (1996).

[16] W. M. Kloet, W.-T. Chiang, and F. Tabakin, Few-Body Systems Suppl. **11**, 308 (1999).

[17] A. Titov, M. Fujiwara, and L. T-S.H., Phys. Rev. **C 66**, 0222202 (2002).

[18] D. Keller, Eur. Phys. J. A **53**, 155 (2019).

[19] J. Ballam and others (ABBHHM Coll.), Phys. Rev. **D7**, 3150 (1973).

[20] R. W. Clift and others (LAMP. Coll.), Phys. Rev. **B72**, 144 (1977).

[21] D. P. Barber and others (LAMP2. Coll.), Z. Phys. **C26**, 343 (1984).

[22] J. Barth and others (SAPHIR Coll.), Eur. Phys. J. **A18**, 117 (2003).

[23] M. Williams and others (CLAS Coll.), Phys. Rev. **C80**, 065208 (2009).

[24] P. S. K. Schilling and G. Wolf, Nucl. Phys **B15**, 397 (1970).

[25] C. S. M. Pichowsky and F. Tabakin, Phys. Rev. **C53**, 593 (1996).

[26] A. I. T. Y. Oh and T.-S. H. Lee, Phys. Rev. **C63**, 025201 (2001).

[27] W. de Boer, Cern Report CERN-74-11 (1974).

[28] P. Hautle, PhD. Thesis.

[29] P. Hautle *et al.*, Nucl.Instrum.Meth. **A356**, 108 (1995).